Supporting Information

A Switchable-Transparency Eutectogel Enabled by Multiple Dynamic Interactions for Smart Display Applications

Phuc Khanh Lam,[‡a] Trung Hieu Vo,[‡b,c] Hai Do-Quoc Nguyen,[d] Hung-Yi Chi,[e] Yu-Jane Sheng[e*] and Heng-Kwong Tsao[b*]

[a]Department of Applied Physics and Chemistry, University of Taipei, Taipei 10048, Taiwan

[b]Department of Chemical and Materials Engineering, National Central University, Taoyuan, 32001, Taiwan

[c]Department of Chemistry, National Central University, Taoyuan, 32001, Taiwan, Taoyuan, 32001, Taiwan

[d]School of Biomedical Engineering, International University, Ho Chi Minh City 700000, Vietnam

[e]Department of Chemical Engineering, National Taiwan University, Taipei 10617, Taiwan

[*]*Corresponding author. E-mail address: hktsao@cc.ncu.edu.tw (H. -K. Tsao); yjsheng@ntu.edu (Y. -J. Sheng)*

‡ These authors contributed equally to this work.

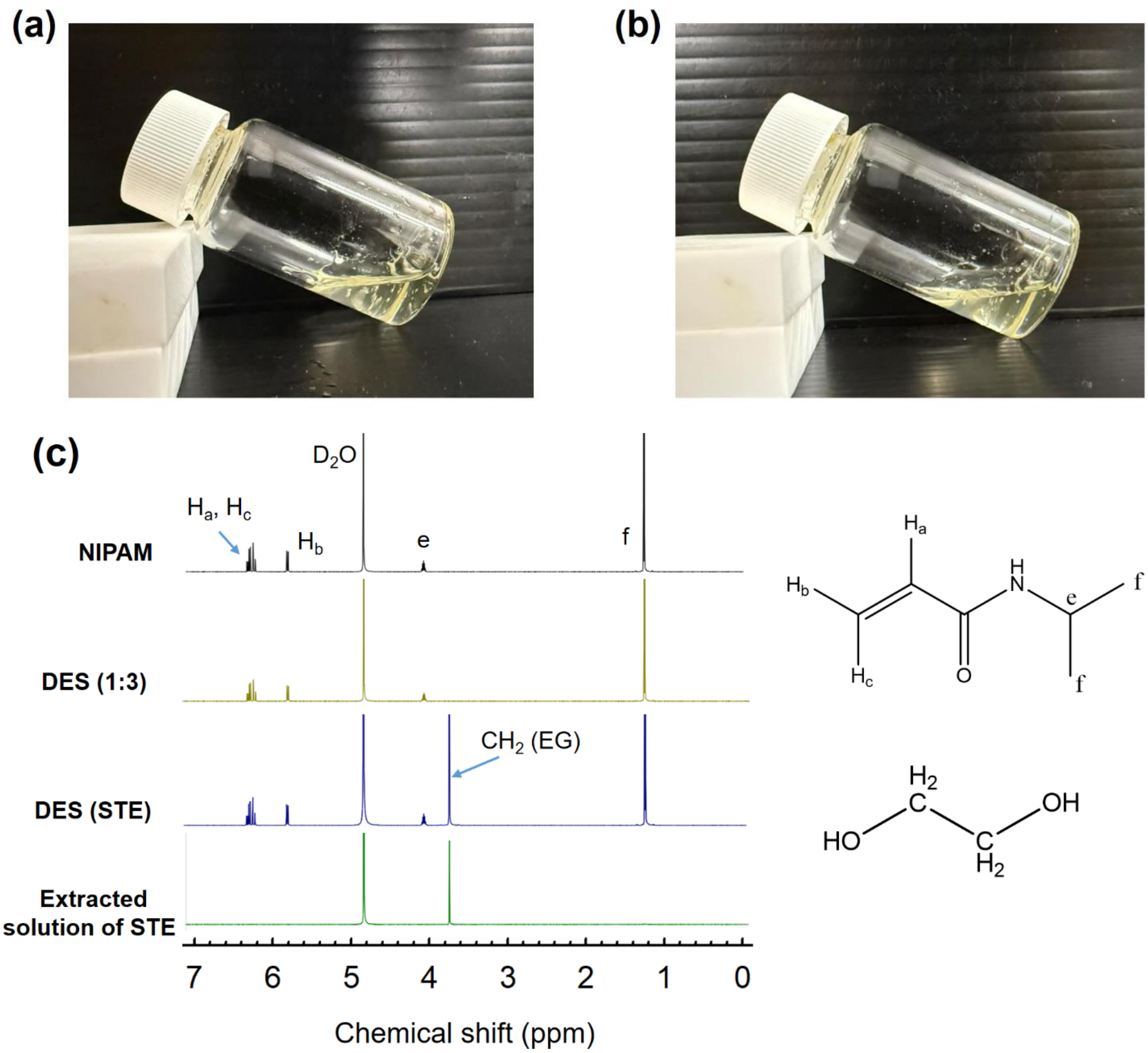

Figure S1. Photograph of type IV DESs with molar ratios of (a) 1:2 and (b) 1:4. (c) NMR spectra of NIPAM, DES (1:3), DES (STE), and the extracted solution of STE in D_2O.

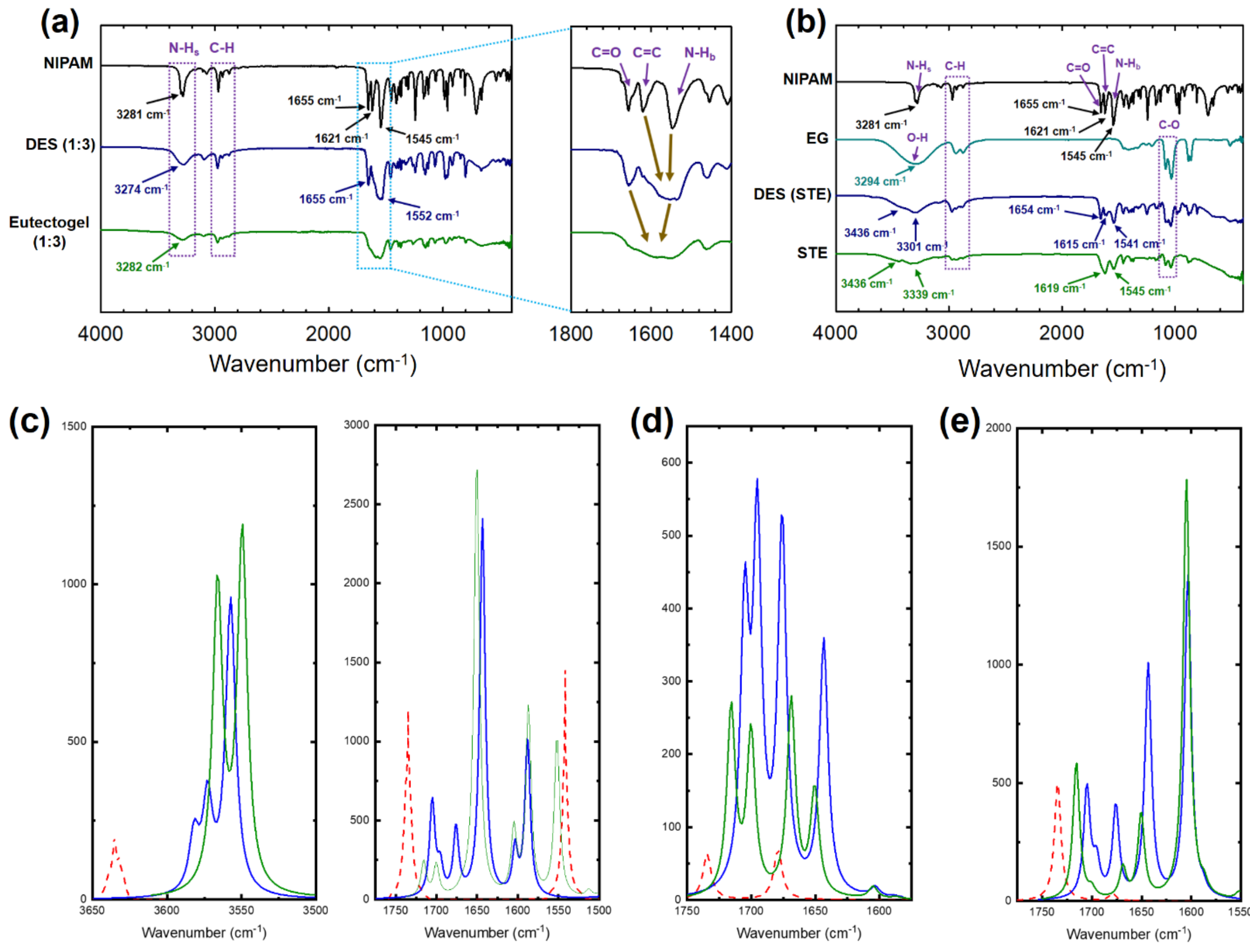

Figure S2. (a, b) FTIR spectra of NIPAM, DES (1:3), eutectogel (1:3), EG, DES (STE), and STE. DFT-calculated IR spectra of (c) N–H, (d) C=C, and (e) C=O, comparing pure NIPAM with the DES. The red dashed line shows pure NIPAM, while the blue and green lines show configurations (d) and (e), respectively.

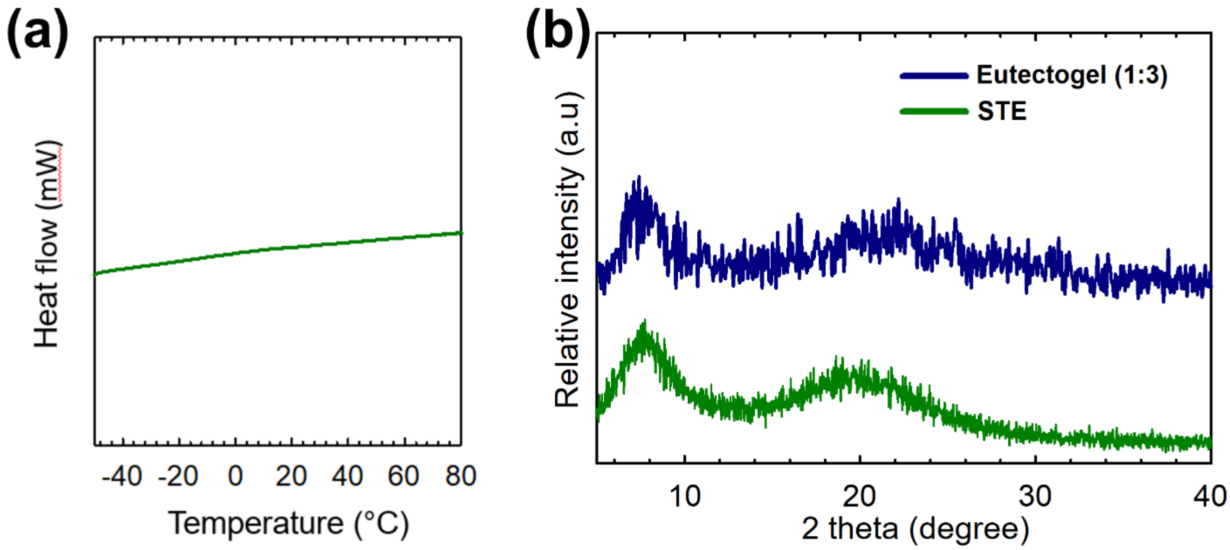

Figure S3. (a) DSC thermogram of the STE from −50 to 80 °C. (b) PXRD patterns of the freeze-dried eutectogel (1:3) and STE. Note that the eutectogel (STE) is prepared using a DES (1:3) containing 35 wt% EG and 5 wt% LiCl.

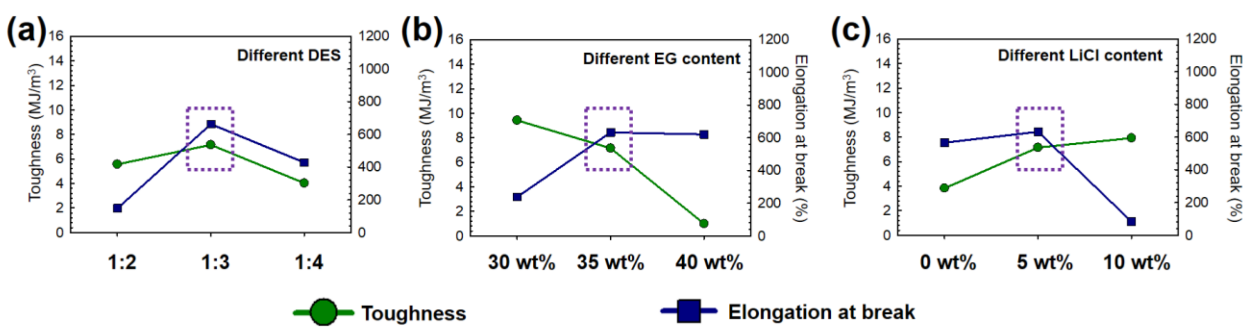

Figure S4. Toughness and elongation at break of the eutectogel formed with: (a) different DESs, 35 wt% EG, and 5 wt% LiCl; (b) DES (1:3) with varying EG contents and 5 wt% LiCl; and (c) DES (1:3), 35 wt% EG, and different LiCl contents.

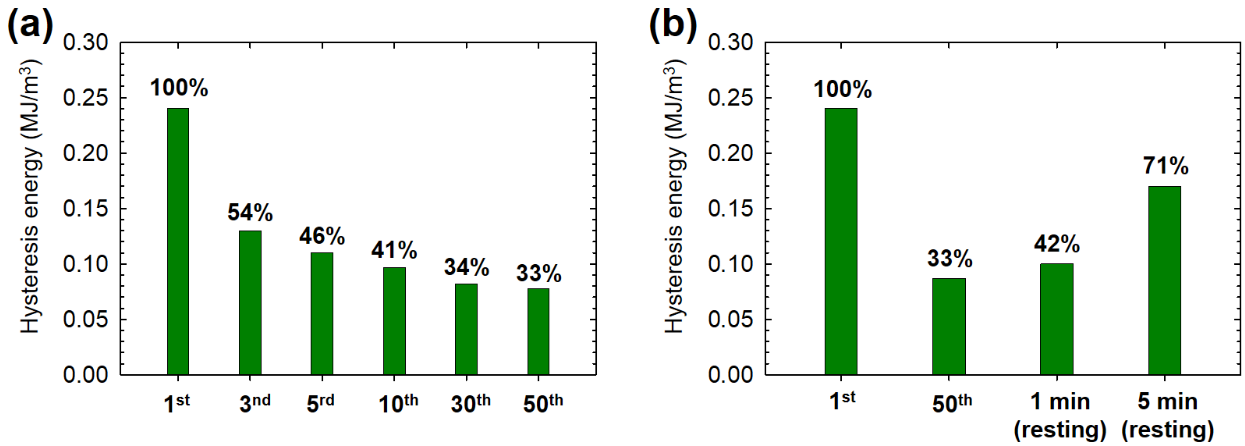

Figure S5. Hysteresis energy of the STE (a) under different loading–unloading cycles and (b) at varying resting times. Note that the eutectogel (STE) uses component of DES (1:3) with 35 wt% EG and 5 wt% LiCl.

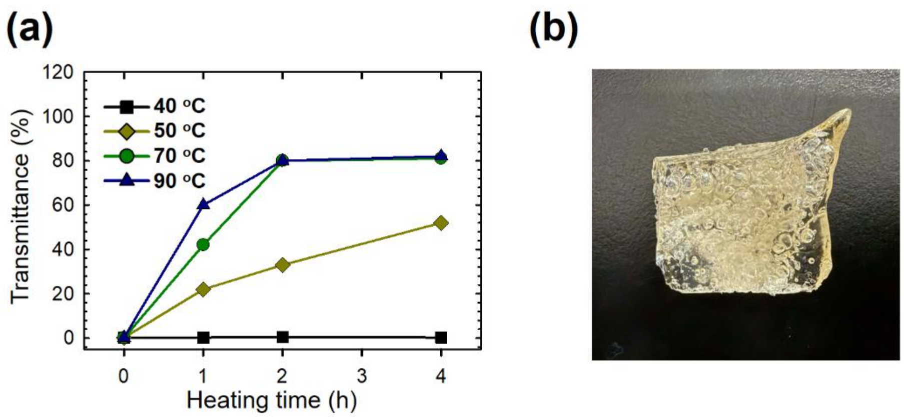

Figure S6. (a) UV-Vis spectra of the STE after heating at different temperatures and for various time periods. (b) Photograph of eutectogel (1:3). Note that the eutectogel (1:3) remains unchanged after heating at 70℃ for 2 hours, indicating no switchable transparency behavior.

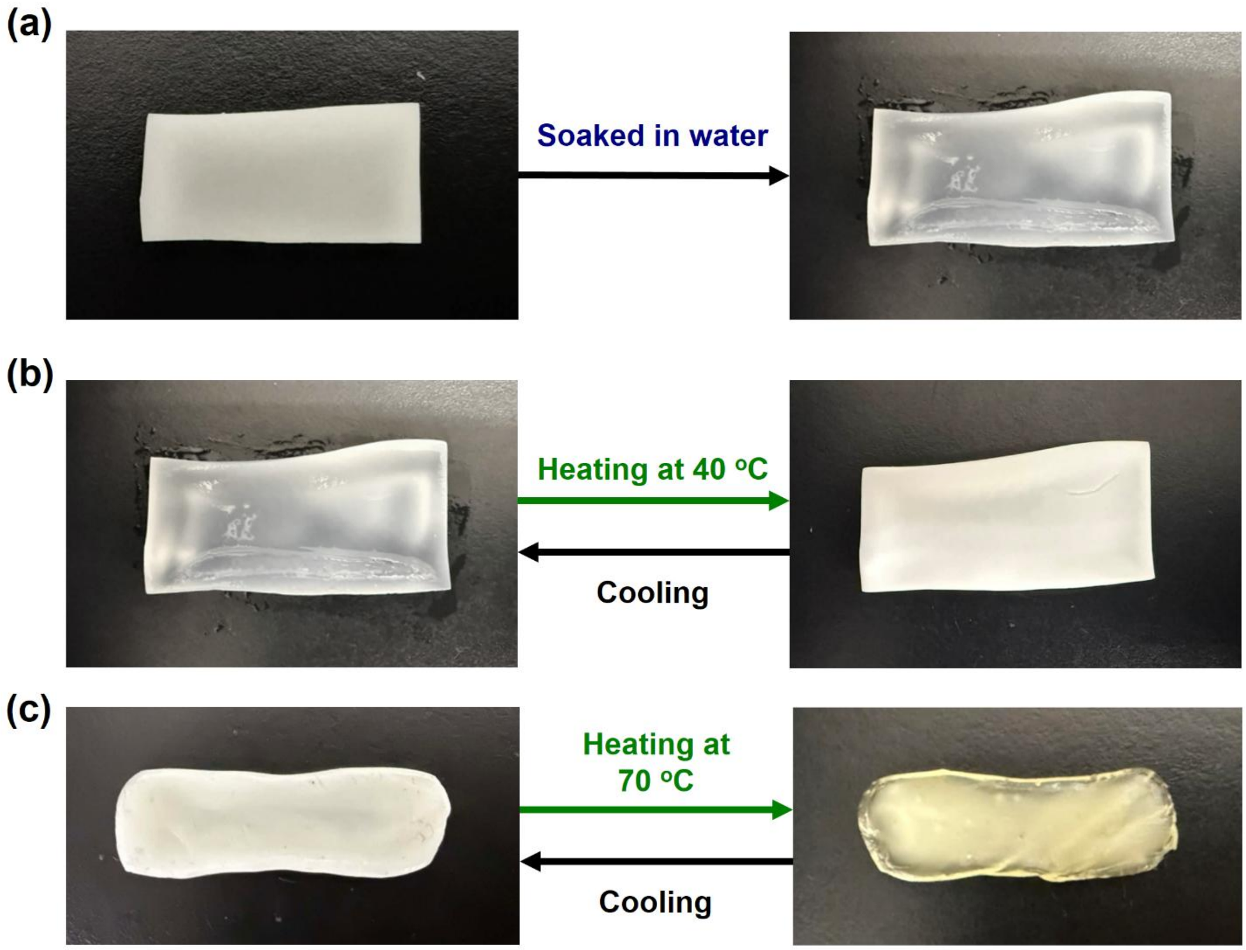

Figure S7. (a) Photograph of the hydrogel, which is STE after being soaked in water. (b) Photograph showing the LCST behavior of the hydrogel before and after the heating-cooling cycle (heated at 40℃ for 15 minutes). (c) Photograph showing the UCST behavior of the gel (without $ZnCl_2$) before and after the heating-cooling cycle (heated at 70℃ for 2 hours). Note that the water-exchange process is similar to the sample preparation used for SEM and XRD, except that no freeze-drying is applied. The hydrogel increases in size by approximately 1.5 times compared to the eutectogel due to swelling after the complete water-exchange process, whereas the sample size in (b) and (c) remains nearly unchanged after the heating and cooling processes.

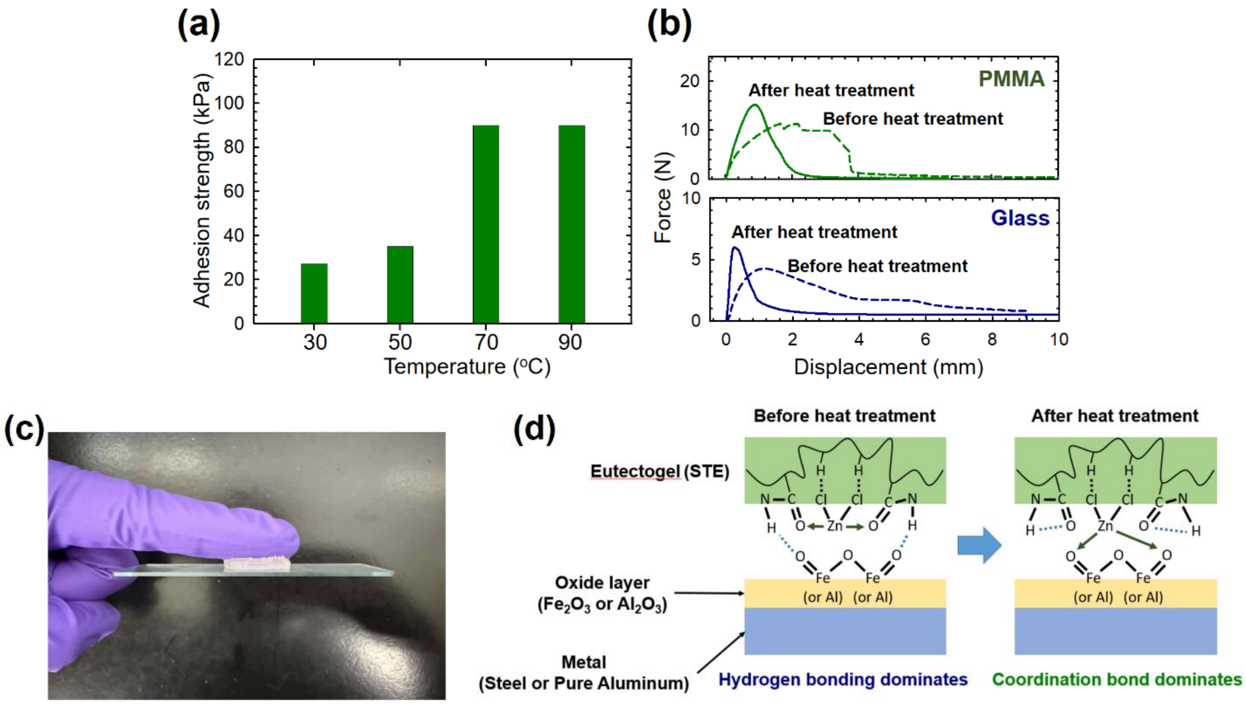

Figure S8. (a) Adhesion strength of the STE on steel substrates after heat treatment at various temperatures. (b) Force-displacement curves on PMMA and glass substrates before and after heat treatment at 70 °C for 2h in shear adhesion tests. (c) Photograph of the STE adhering to a glass substrate and being lifted by a finger. (d) Proposed mechanism for the temperature-enhanced adhesion strength.

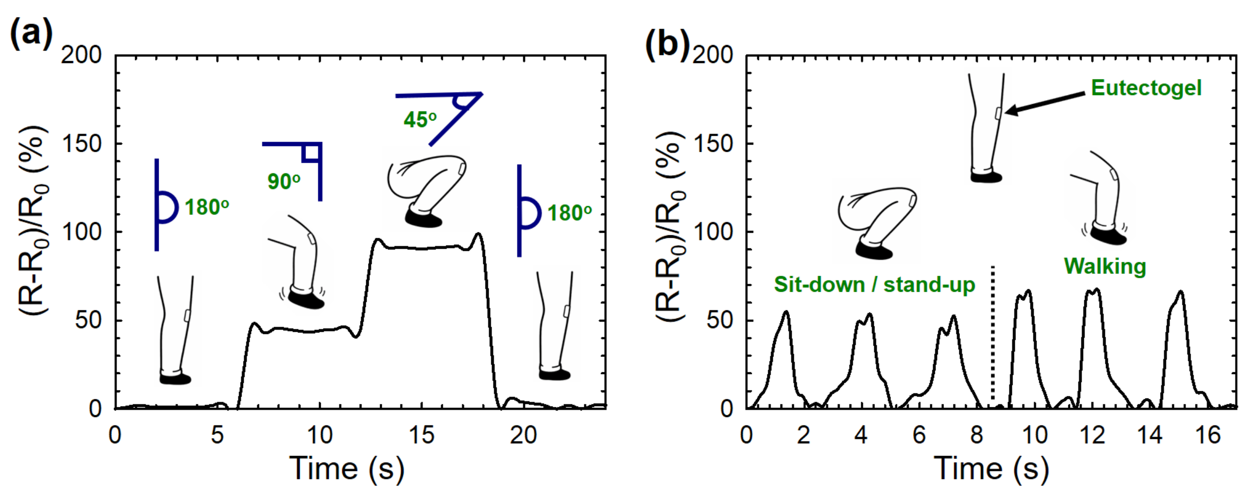

Figure S9. Relative resistance changes (a) at different knee bending angles and (b) during sitting down/standing up and walking movements.

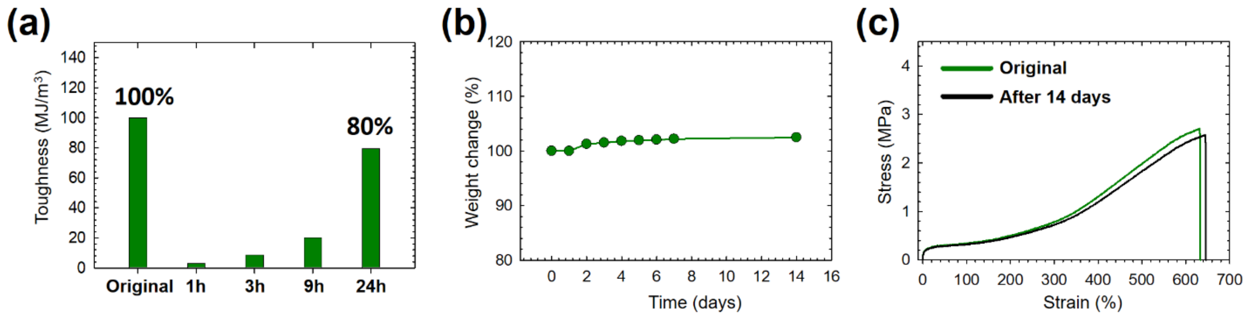

Figure S10. (a) Toughness of the STE after different self-healing times. (b) Weight change of the STE over time. (c) Stress–strain curves after 14 days compared with the original.